Built-in electric field effect on cyclotron mass of magnetopolarons in a wurtzite $In_xGa_{1-x}N/GaN$ quantum well*

Zhao Feng-Qi(赵凤岐)[a)†] and Yong Mei(咏 梅)[b)]

[a)] *College of Physics and Electronic Information, Inner Mongolia Normal University, Inner Mongolia Key Laboratory for Physics and Chemistry of Functional Materials, Hohhot* 010022, *China*

[b)] *Division of Science and Technology, Inner Mongolia Normal University, Hohhot* 010022, *China*

(Received 2 February 2012; revised manuscript received 2 April 2012)

The cyclotron mass of magnetopolarons in wurtzite $In_xGa_{1-x}N/GaN$ quantum well is studied in the presence of an external magnetic field by using the Larsen perturbation method. The effects of the built-in electric field and different phonon modes including interface, confined and half-space phonon modes are considered in our calculation. The results for a zinc-blende quantum well are also given for comparison. It is found that the main contribution to the transition energy comes from half-space and interface phonon modes when the well width is very small while the confined modes play a more important role in a wider well due to the location of the electron wave function. As the well width increases, the cyclotron mass of magnetopolarons first increases to a maximum and then decreases either with or without the built-in electric field in the wurtzite structure and the built-in electric field slightly reduces the cyclotron mass. The variation of cyclotron mass in a zinc-blende structure is similar to that in a wurtzite structure. With the increase of external magnetic field, the cyclotron mass of polarons almost linearly increases. The cyclotron frequency of magnetopolarons is also discussed.

Keywords: wurtzite quantum well, built-in electric field, magnetopolaron, cyclotron mass

PACS: 71.38.–k, 63.20.kr, 73.21.Fg **DOI:** 10.1088/1674-1056/21/10/107103

1. Introduction

The interaction of electrons with optical phonons in a quasi-two-dimensional system has been studied both theoretically and experimentally for many years because of its importance with respect to both device application and fundamental physics. The investigation of the cyclotron resonance (CR) of polarons can be usually performed by using the one-electron approximation at a sufficiently low density of electrons. Some authors adopted a bulk phonon approximation to simplify the complicated electron–phonon interaction.[1−4] However these studies overexaggerated the phonon influence due to the dimensional effect of polarons. Kong *et al.*[5] and Hu *et al.*[6] discussed the ground states and CR of interface magnetopolarons in heterojunctions by considering the effect of bulk longitudinal optical (LO) phonons and a single branch of effective interface (IF) optical phonons. In a previous paper,[7] we considered all of the bulk LO phonons and IF phonons to study the polaron CR in single quantum wells (QWs). Later on, Hai and Peeters[8] investigated the magnetopolaron effect in parabolic QWs with a tilted magnetic field. Using the Green's function approach, some authors[9,10] also studied the resonant magnetopolaron effect in QWs at a high electron density. However, to our knowledge, there is still a lack of study on the cyclotron mass and frequency of magnetopolarons in wurtzite heterostructures.

Low-dimensional heterostructures made of wurtzite group-III nitride semiconductors such as AlN, GaN, InN, and their alloys have recently contributed a great deal to the progress of the fabrication of a wide variety of optoelectronic devices, such as high-brightness ultraviolet/blue/green light-emitting diodes, laser diodes, and ultraviolet photodetectors.[11−17] Compared to a zinc-blende

*Project supported by the National Natural Science Foundation of China (Grant No. 10964007) and the Natural Science Foundation of Inner Mongolia, China (Grant No. 2009MS0110).

†Corresponding author. E-mail: fqzhao@imnu.edu.cn

© 2012 Chinese Physical Society and IOP Publishing Ltd

structure, there are some unique properties in wurtzite QWs mainly because of the lower symmetry of the unit-cell structure and the residual strain at the heterointerface. A strong built-in electric field (BEF) produced by the spontaneous and strain-induced piezoelectric polarization is present in nitride heterostructures and greatly affects the spatial quantization of the electron states.[18−21] Due to the anisotropy of the wurtzite structure, there are much more distinct phonon branches and extraordinary phonon modes may even exist in this structure, caused by the mixing of the longitudinal and transversal optical (TO) modes. The dispersion relations of various phonon modes[22] and the corresponding electron–optical phonon Fröhlich Hamiltonians[23] were derived within the macroscopic dielectric continuum model and Loudon's uniaxial model. These studies are helpful for discussing in detail the electron–optical phonon interaction in wurtzite heterostructures. This also gives us an impetus to investigate polaron CR in a wurtzite QW structure. The effects of a polaron in a wurtzite GaN/$Al_xGa_{1-x}N$ QW had been studied within the framework of the electron–optical phonon interaction Hamiltonian.[24,25] However less research has been done on the magnetopolaron in the wurtzite nitride QW, to our knowledge.

In this work, we adopt the Larsen perturbation method[26,27] to investigate the cyclotron mass and the cyclotron frequency of the magnetopolaron in a wurtzite $In_xGa_{1-x}N$/GaN QW with an external magnetic field. The BEF effect and the contributions from different phonon modes, namely, IF, confined (CF), half-space (HS) modes, are taken into account in our calculation.

2. Model and calculation

We consider a wurtzite $In_xGa_{1-x}N$/GaN QW structure for which the well material $In_xGa_{1-x}N$ is denoted by "$\lambda = 1$" and is located between $z = \pm d/2$, while the barrier material GaN is denoted by "$\lambda = 2$" and fills up the region $|z| > d/2$. In general, the z axis is taken to be parallel to the direction of the crystal growth and the x–y plane parallel to the interface. The coordinate origin is taken to be at the midpoint of the well. By using the effective-mass approximation and considering the anisotropy of effective mass and the interactions from the CF, IF, and HS phonons, the Hamiltonian of the electron–optical phonon system can be written as

$$H = H_{xy} + H_z + \sum_{\boldsymbol{w}j} \hbar\omega a_j^{\dagger}(\boldsymbol{w}) a_j(\boldsymbol{w}) + H_{\text{e-ph}}, \quad (1)$$

with

$$H_{xy} = \frac{1}{2m_{\lambda\perp}}(p_x + eBy)^2 + \frac{p_y^2}{2m_{\lambda\perp}},$$
$$H_z = \frac{p_z^2}{2m_{\lambda z}} + V(z), \quad (2)$$

where $m_\lambda = (m_{\lambda\perp}, m_{\lambda z})$ is the position-dependent effective mass of an electron; e is the absolute value of the electron charge; B is the magnetic field strength; $a_j^{\dagger}(\boldsymbol{w})$ ($a_j(\boldsymbol{w})$) is the creation (annihilation) operator of optical phonons with wave vector $\boldsymbol{w}$ ($\boldsymbol{w} = (\boldsymbol{q}, k_{\lambda z})$ for CF and HS phonon modes, $\boldsymbol{w} = \boldsymbol{q}$ for IF phonon modes), and frequency ω; $j = \{l, \beta\}$ with the mode index l as the symmetric and antisymmetric phonon modes, β as the CF, HS, and IF phonon modes in LO-like and TO-like phonon frequency regions; $V(z)$ is the potential height experienced by the electron, which can be given as

$$V(z) = \begin{cases} V_0 - eFd/2, & z < -d/2, \\ -eFz, & |z| \le d/2, \\ V_0 + eFd/2, & z > d/2, \end{cases} \quad (3)$$

where $V_0 = 0.7\Delta E_{\text{g}}$, $\Delta E_{\text{g}} = x(E_{\text{g}}(\text{GaN}) - E_{\text{g}}(\text{InN})) + bx(1-x)$ with bowing parameter b taken to be 1.4 eV,[28,29] and F is the BEF taken to be 1.56 MV/cm.[18] The last term in Eq. (1) is the Hamiltonian of the interaction between electrons and phonons. It can be generally written as

$$H_{\text{e-ph}} = \sum_{\boldsymbol{w}j} \left[g_{jw}(z) \exp(-\mathrm{i}\boldsymbol{q}\cdot\boldsymbol{\rho}) a_j^{\dagger}(\boldsymbol{w}) + \text{h.c} \right]. \quad (4)$$

For the symmetric CF modes, the coupling function $g_{jw}(z)$ in Eq. (4) is determined by the following equation:[23]

$$g_{\text{S,CF}}(z) = -\mathrm{i}[4\pi\hbar e^2 L^{-2}/((\partial/\partial\omega)(\varepsilon_{1\perp}q^2 + \varepsilon_{1z}k_{1m}^2)d/2 - 2q(\partial/\partial\omega)f_s(\omega)\cos(k_{1m}d/2))]^{1/2}\chi_{jS}(z), \quad (5)$$

and

$$\chi_{jS}(z) = \begin{cases} \cos(k_{1m}z), & (|z| < d/2), \\ \cos(k_{1m}d/2)\exp(-\kappa_2(|z| - d/2)), & (|z| \ge d/2), \end{cases} \quad (6)$$

where $f_s(\omega) = \text{sgn}(\varepsilon_{1z})\sqrt{-\varepsilon_{1\perp}(\omega)\varepsilon_{1z}(\omega)}\sin(k_{1m}d/2) - \text{sgn}(\varepsilon_{2z})\sqrt{\varepsilon_{2\perp}(\omega)\varepsilon_{2z}(\omega)}\cos(k_{1m}d/2)$, k_{1m} can be

determined by the equation $\varepsilon_{1z}k_{1m}\sin(k_{1m}d/2) - \varepsilon_{2z}k_2\cos(k_{1m}d/2) = 0$ in a range of $2m\pi/d < k_{1m} < 2(m+1)\pi/d$, m runs over the series of confined modes, and L^2 is the interface area of quantum well.

For the antisymmetric CF modes, the coupling function $g_{jw}(z)$ in Eq. (4) is determined by the following equation:[23]

$$\begin{aligned} & g_{\mathrm{AS,CF}}(z) \\ = & -\mathrm{i}[4\pi\hbar e^2 L^{-2}/((\partial/\partial\omega)(\varepsilon_{1\perp}q^2+\varepsilon_{1z}k_{1m}^2)d/2 \\ & - 2q(\partial/\partial\omega)f_a(\omega)\sin(k_{1m}d/2))]^{1/2}\chi_{jA}(z), \end{aligned} \quad (7)$$

and

$$\begin{aligned} & \chi_{jA}(z) \\ = & \begin{cases} \sin(k_{1m}z), & |z| < d/2, \\ \mathrm{sgn}(z)\sin(k_{1m}d/2) & \\ \quad \times\exp(-\kappa_2(|z|-d/2)), & |z| \geq d/2, \end{cases} \end{aligned} \quad (8)$$

where $f_a(\omega) = \mathrm{sgn}(\varepsilon_{1z})\sqrt{-\varepsilon_{1\perp}(\omega)\varepsilon_{1z}(\omega)}\cos(k_{1m}d/2) + \mathrm{sgn}(\varepsilon_{2z})\sqrt{\varepsilon_{2\perp}(\omega)\varepsilon_{2z}(\omega)}\sin(k_{1m}d/2)$, k_{1m} can be determined by the equation $\varepsilon_{1z}k_{1m}\cos(k_{1m}d/2) + \varepsilon_{2z}k_2\sin(k_{1m}d/2) = 0$ in a range of $(2m-1)\pi/d < k_{1m} < (2m+1)\pi/d$, $(m = 1, 2, 3, \ldots)$. Similar to the CF modes, the HS and IF phonon modes are expressed in Ref. [23].

The direction-dependent dielectric functions, $\varepsilon_{\lambda\perp}(\omega)$ and $\varepsilon_{\lambda z}(\omega)$, are given by

$$\begin{aligned} \varepsilon_{\lambda\perp}(\omega) &= \varepsilon_{\lambda\perp}^{\infty}\frac{\omega^2-\omega_{\lambda\perp L}^2}{\omega^2-\omega_{\lambda\perp}^2}, \\ \varepsilon_{\lambda z}(\omega) &= \varepsilon_{\lambda z}^{\infty}\frac{\omega^2-\omega_{\lambda zL}^2}{\omega^2-\omega_{\lambda z}^2}. \end{aligned} \quad (9)$$

The values of phonon frequency ω for CF mode are obtained from $\varepsilon_{\lambda\perp}(\omega)\sin^2\theta_\lambda + \varepsilon_{\lambda z}(\omega)\cos^2\theta_\lambda = 0$ with a proper application of parameters for material 1(2). θ_λ is an angle between $\boldsymbol{w}$ and z axis.

The Hamiltonian in Eq. (1) cannot be solved exactly. We use the perturbation method to deal with the electron–phonon interaction. Then, the Hamiltonian is written into two parts as

$$H = H_0 + H_{\mathrm{I}}, \quad (10)$$

where $H_0 = H_{xy} + H_z + \sum_{\boldsymbol{w}j}\hbar\omega a_j^{\dagger}(\boldsymbol{w})a_j(\boldsymbol{w})$ is the unperturbed part, and $H_{\mathrm{I}} = H_{\text{e-ph}}$ is perturbation part. The energy levels and the corresponding wavefunctions for H_{xy} can be easily written as

$$E_n = \left(n+\frac{1}{2}\right)\hbar\omega_{\mathrm{c}},\ n = 0, 1, 2, \ldots, \quad (11)$$

$$\begin{aligned} \varphi_n(p_x, y) = & N_n\exp[\mathrm{i}p_x x/\hbar - eB(y-y_0)^2/\hbar] \\ & \times H_n[(eB/\hbar)^{1/2}(y-y_0)], \end{aligned} \quad (12)$$

where N_n is the normalization constant and $\omega_{\mathrm{c}} = eB/m_{\lambda\perp}$. The eigenvalues and eigenfunctions for H_z are assumed to be E_i and $\varphi_i(z)$ with $i = 1, 2, 3, \ldots$. Then the unperturbed energy levels for the Hamiltonian H_0 are given by

$$E_{niQ}^0 = E_i + \left(n+\frac{1}{2}\right)\hbar\omega_{\mathrm{c}} + \sum_{\boldsymbol{w}j}\hbar\omega Q_{wj}, \quad (13)$$

where Q_{wj} is the phonon number, and the corresponding wavefunction is

$$|\psi_{niQ}\rangle = |\varphi_n\rangle\,|\phi_i\rangle\,|Q_{wj}\rangle\,. \quad (14)$$

It may be seen from Eq. (13) that the energy difference of the electron in z direction is much larger than the energy difference of the electron in x–y plane and the probability of the electron excited from the ground state ($i = 1$) in the z direction can be neglected. Therefore, we assume that the electron always lies in the first subband ($i = 1$) in the QW, and carry out only the second-order perturbation calculation for the motion in the x–y plane. Furthermore, we focus on the discussion of the zero-phonon state (low temperature limit). Finally, the perturbed energy will be averaged over the wavefunction $\phi_i(z)$ to obtain the energy of the magnetopolaron.

It is clearly seen from Eq. (4) that the first-order perturbation energy is zero. The second-order perturbation energy for the Landau ground state ($n = 0$) level can be written by

$$\Delta E_0^{(2)} = \sum_{\boldsymbol{w}jn'}\frac{|\langle\varphi_{n'}(p_x)|\,\langle 1_{wj}|\,H_I\,|0\rangle\,|\varphi_0(0)\rangle|^2}{E_{n'iQ}^{(0)} - E_{0i0}^{(0)}}. \quad (15)$$

Following Larsen,[26,27] the energy denominators in Eq. (15) can be written as $n'\gamma^2 + 1$, where $\gamma^2 = \omega_{\mathrm{c}}/\omega$. By evaluating the matrix elements in Eq. (15), the contribution of the phonon modes to the energy of the magnetopolaron can be given as

$$\Delta E_0^{(2)} = \sum_{n'}\frac{|I_{n'}|^2}{n'\gamma^2+1}\sum_{\boldsymbol{w}j}\frac{|g_{jw}(z)|^2}{\hbar\omega}, \quad (16)$$

where

$$\begin{aligned} I_{n'} = & \int_{-\infty}^{\infty}\mathrm{d}y N_{n'}H_{n'}[(eB/\hbar)^{1/2}(y-y_0)] \\ & \times\exp\{-eB[(y-y_0)^2+y^2]/2\hbar - \mathrm{i}yk_z\}. \end{aligned} \quad (17)$$

Using Larsen's method[26,27] to evaluate the summation and replacing the summation over $\boldsymbol{w}$ by an integration, and expecting the value of the contribution in the wavefunction $\phi_1(z)$, Eq. (16) can be given as

$$\begin{aligned}&\langle\phi_1(z)|\,\Delta E_0^{(2)}\,|\phi_1(z)\rangle\\&=\sum_{\boldsymbol{w}j}\langle\phi_1(z)|\,\frac{|g_{jw}(z)|^2}{\hbar\omega}\,|\phi_1(z)\rangle\left[\frac{1}{1+t^2}+\frac{\gamma^2t^2}{(1+t^2)^3}\right.\\&\left.+\gamma^4t^2\left(-\frac{1}{(1+t^2)^4}+\frac{3t^2}{(1+t^2)^5}\right)+\cdots\right],\end{aligned}\tag{18}$$

where $t=\sqrt{\hbar/2m_{1\perp}\omega}q$. Finally, we obtain the ground-state energy of the magnetopolaron in the QW as

$$E_0^*=E_1+\frac{1}{2}\hbar\omega_{\rm c}+\langle\phi_1(z)|\,\Delta E_0^{(2)}\,|\phi_1(z\rangle\,.\tag{19}$$

The calculation of Landau excited state is the same as that for the ground state but $n=0$ is replaced by $n=1$. The contribution of the phonon modes to the first excited state energy of the magnetopolaron can be given as

$$\begin{aligned}&\langle\phi_1(z)|\,\Delta E_1^{(2)}\,|\phi_1(z)\rangle\\&=\sum_{\boldsymbol{w}j}\langle\phi_1(z)|\,\frac{|g_{jw}(z)|^2}{\hbar\omega}\,|\phi_1(z)\rangle\left[\frac{1}{1+t^2}+\frac{3\gamma^2t^2}{(1+t^2)^3}\right.\\&\left.+\gamma^4t^2\left(-\frac{1}{(1+t^2)^4}+\frac{15t^2}{(1+t^2)^5}\right)+\cdots\right],\end{aligned}\tag{20}$$

and the first excited state energy of the magnetopolaron in the QW is written as

$$E_1^*=E_1+\frac{3}{2}\hbar\omega_{\rm c}+\langle\phi_1(z)|\,\Delta E_1^{(??)}\,|\phi_1(z\rangle\,.\tag{21}$$

The cyclotron frequency ($\omega_{\rm c}^*$) of the magnetopolaron is determined by the difference (transition energy $\Delta E=E_1^*-E_0^*$) between the energy of the first excited state ($n=1$) and ground state ($n=0$)

$$\omega_{\rm c}^*=(E_1^*-E_0^*)/\hbar,\tag{22}$$

and the cyclotron mass (m^*) is given by

$$m*=\omega_{\rm c}m_{1\perp}/\omega_{\rm c}^*.\tag{23}$$

3. Numerical results and discussion

We numerically compute the cyclotron mass and cyclotron frequency of magnetopolarons in wurtzite $In_{0.19}Ga_{0.81}N$/GaN QWs. The parameters used in the calculation are listed in Tables 1 and 2, and the parameters of $In_xGa_{1-x}N$ are obtained by the effective phonon-mode approximation.[37] The corresponding results are plotted in Figs. 1–4. The results in the zinc-blende QWs obtained in a similar way are also given for comparison.

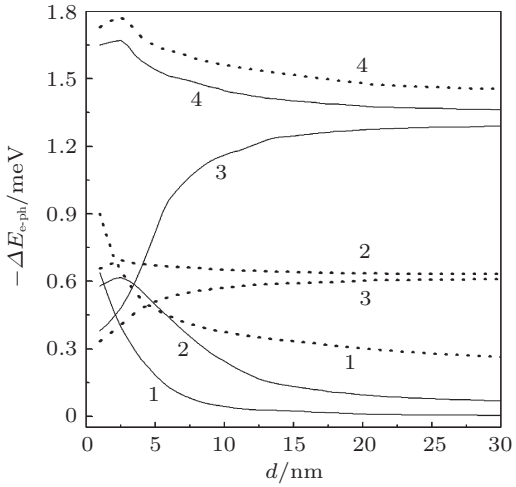


Fig. 1. Phonon contributions to the transition energy each as a function of well width d in wurtzite $In_{0.19}Ga_{0.81}N$/GaN QWs without (solid lines) and with (dashed lines) a BEF. The energy shifts $\Delta E_{\rm HS}$, $\Delta E_{\rm IF}$, and $\Delta E_{\rm CF}$ separately contributed from the HS, IF, and CF phonon modes and the total energy shift $\Delta E_{\rm Total}$ are denoted as "1", "2" , "3", and "4" respectively. Here, B is fixed at 16 T.

Figure 1 shows the phonon contributions to the transition energy from the HS, IF, and CF phonon modes and their summation each as a function of well width d in wurtzite $In_{0.19}Ga_{0.81}N$/GaN QWs without (solid lines) and with (dashed lines) a BEF. It can be found that the main contribution comes from HS and IF phonon modes when the well width is very small while the CF modes play a more important role in a wider well due to the location of the electron wave function. Either with or without a BEF, as d increases, $\Delta E_{\rm HS}$ decreases and reaches a constant, $\Delta E_{\rm IF}$ first increases and then decreases, whereas $\Delta E_{\rm CF}$ increases to a constant, which leads $\Delta E_{\rm Total}$ to first increase to a maximum and then gradually decrease and approach to a constant. The difference between the values of $\Delta E_{\rm Total}$ without and with a BEF is about 0.11 meV. It should be mentioned that the contribution from the antisymmetric part of each mode cannot be neglected in an actual situation since the BEF breaks down the symmetry of the well potential, thereby making the electrons always approach the left boundary of the interface. According to our calculation, the TO-like phonons always make a negligibly small contribution to the transition energy compared with LO-like phonons, e.g., when $d=20$ nm, the contribution from TO-like phonons is about 0.1 meV and is 1.6 meV from LO-like phonons.

Table 1. Parameters for wurtzite QWs used in the calculation. The electron effective mass, phonon frequency, and the band gap are in units of the electron rest mass m_e, meV, and eV, respectively.

Materials	$m_\perp = m_z$	$\varepsilon_\perp^\infty$	ε_z^∞	$\omega_\perp$	ω_z	$\omega_{\perp L}$	ω_{zL}	E_g
GaN	0.20[30]	5.70[31]	5.70[31]	69.56[32]	66.08[32]	92.12[32]	91.13[32]	3.51[30]
InN	0.12[30]	8.40[33]	8.40[33]	59.02[34]	55.43[34]	73.53[34]	72.64[34]	1.99[30]

Table 2. Parameters for zinc-blende QWs used in the calculation.

Materials	m	ε^∞	ω_{LO}	ω_{TO}	E_g
GaN	0.15[30]	5.70[31]	90.63[35]	68.32[35]	3.30[30]
InN	0.10[36]	8.40[33]	72.66[34]	58.52[34]	1.94[30]

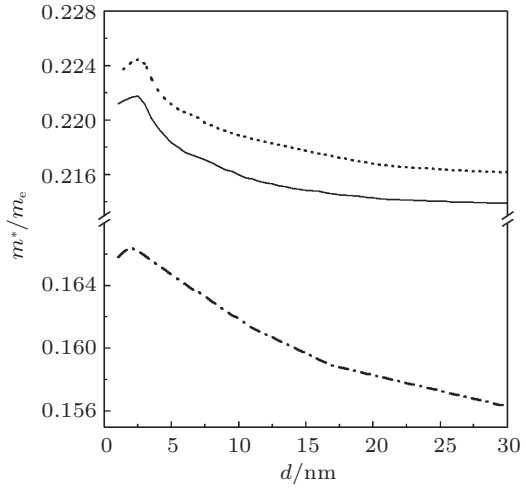


Fig. 2. Curves of the cyclotron mass of magnetopolarons versus well width d in wurtzite $In_{0.19}Ga_{0.81}N$/GaN QW with (dot lines) and without a BEF (solid lines), and in zinc-blende QW (dashed dot lines). Here, B is fixed at 16 T.

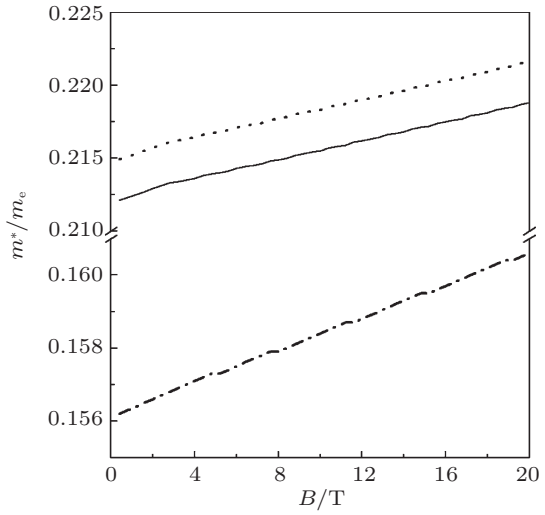


Fig. 3. Curves of cyclotron mass of magnetopolarons versus magnetic field B in specified wurtzite $In_{0.19}Ga_{0.81}N$/GaN QW with (dot lines) and without a BEF (solid lines), and in zinc-blende QW (dashed dot lines). Here, d is chosen to be 15 nm.

Figure 2 gives the curves of the cyclotron mass of magnetopolarons m^* versus well width d for different values of magnetic field B. As d increases, m^* first increases to a maximum then decreases either with or without the BEF due to the quantum confinement of electrons. m^* is scarcely influenced by the BEF, since the BEF has less influence on the difference between two energy levels of magnetopolarons although the energy levels are greatly shifted by the BEF. As for the zinc-blende structure, the change of m^* is similar to that in the wurtzite structure but the value of m^* is smaller. To clearly see the influence of the magnetic field, we plot the curves of the cyclotron mass of magnetopolarons m^* versus B for $d = 15$ nm in Fig. 3. It is found that m^* almost linearly increases with B. The results are consistent with those in previous works.[4,7,38]

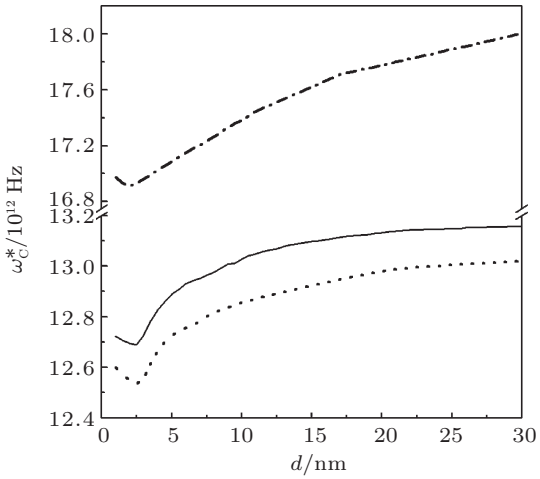


Fig. 4. Curves of cyclotron frequency of magnetopolarons versus well width d in wurtzite $In_{0.19}Ga_{0.81}N$/GaN QWs with (dot lines) and without a BEF (solid lines), and in zinc-blende QWs (dashed dot lines). Here, B is fixed at 16 T.

We also illustrate the curves of cyclotron frequency of magnetopolarons ω_c^* versus well width d for a given magnetic field in Fig. 4. From Eq. (22), one can see that ω_c^* is determined by the transition energy, i.e., the energy difference between the first excited state and ground state. With d increasing, ω_c^* first decreases to a minimum and then increases. The cyclotron frequency in wurtzite structure without the BEF is smaller than that with the BEF since the QW potential is tilted by the BEF to reduce the transition energy. It can also be seen that the cyclotron

frequency in a zinc-blende structure is always larger than that in a wurtzite structure. The variations of the cyclotron frequency of magnetopolarons ω_c^* with magnetic field for a given well width are given in Fig. 5. With magnetic field increasing, the transition energy linearly increases, resulting in an increase of ω_c^*.

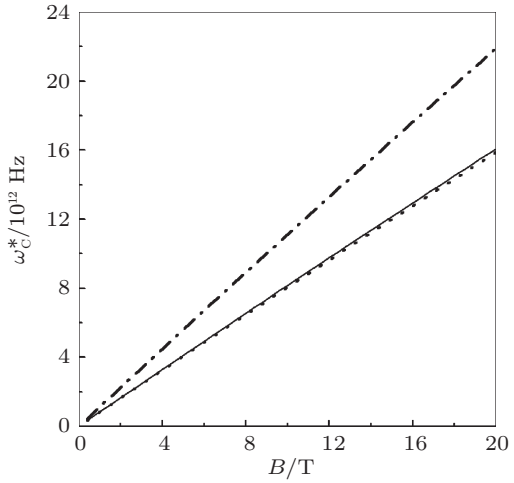


Fig. 5. Variations of the cyclotron frequency of magnetopolarons with magnetic field B in specified wurtzite $In_{0.19}Ga_{0.81}N/GaN$ QW with (dot lines) and without a BEF (solid lines), and in zinc-blende QW (dashed dot lines). Here, d is fixed at 15 nm.

Our results show that the contributions made by the LO-like IF, CF, and HS phonon modes are much larger than those made by the TO-like phonons. The PR phonon modes are not taken into account in our calculation since the LO-like PR modes do not exist in $In_{0.19}Ga_{0.81}N/GaN$ QW due to the condition $\varepsilon_{1\perp}\varepsilon_{1z} < 0$.

4. Conclusion

In the present paper, the cyclotron mass of magnetopolarons in wurtzite $In_xGa_{1-x}N/GaN$ QWs is studied using the Larsen perturbation method. The BEF effect and the contributions from IF, CF, and HS phonon modes are considered in our calculation. The results in the zinc-blende QWs are also included. The main contribution to the transition energy comes from HS and IF phonon modes when the well width is very small while the CF modes play a more important role in a wider well. As the well width increases, the cyclotron mass of magnetopolarons first increases to a maximum then decreases either with or without the BEF in a wurtzite structure, oppositely, the cyclotron frequency first decreases to a minimum and then increases. The variations of the cyclotron mass and frequency of magnetopolarons in a zinc-blende structure are similar to those in a wurtzite structure. With external magnetic field increasing, both the cyclotron mass and frequency almost linearly increase. It is noted that the cyclotron mass and frequency of magnetopolarons are scarcely influenced by the BEF. We hope that the present results are helpful for the relevant experiments and device applications in group-III nitride heterostructures.

References

[1] Das Sarma S 1984 *Phys. Rev. Lett.* **52** 859
[2] Peeters F M, Wu X G and Devreese J T 1986 *Phys. Rev.* B **34** 1160
[3] Larsen D M 1986 *Phys. Rev.* B **33** 799
[4] Osorio F A P, Degani M H and Hipolito O 1988 *Phys. Rev.* B **38** 8477
[5] Kong X J, Wei C W and Gu S W 1989 *Phys. Rev.* B **39** 3230
[6] Hu Z, Wang Y T, Gu S W, Au-Yeung T C and Yeung Y Y 1992 *J. Phys.: Condens. Matter* **4** 5087
[7] Zhao F Q, Wang X and Liang X X 1993 *Phys. Lett.* A **175** 225
[8] Hai G Q and Peeters F M 1999 *Phys. Rev.* B **60** 8984
[9] Li J B, Wei B H and Xia J B 1999 *Physica* B **271** 256
[10] Klimin S N, Fomin V M and Devreese J T 2008 *Phys. Rev.* B **77** 205311
[11] Nykanen H, Mattila P, Suihkonen S, Riikonen J, Quillet E, Honeyer E, Bellessa J and Sopanen M 2011 *J. Appl. Phys.* **109** 08310-1
[12] Wu J Q 2009 *J. Appl. Phys.* **106** 011101
[13] Malyutenko V K, Bolgov S S and Podoltsrv A D 2010 *Appl. Phys. Lett.* **97** 251110
[14] Zhao H and Tansu N 2010 *J. Appl. Phys.* **107** 113110
[15] Yoshida H, Kuwabara M, Yamashita Y, Uchiyama K and Kan H 2010 *Appl. Phys. Lett.* **96** 211122
[16] Belabbes A, de Carvalho L C, Schleife A and Bechstedt F 2011 *Phys. Rev.* B **84** 125108
[17] Chang W L and John A P 2011 *Chin. Phys.* B **20** 077104
[18] Cai J and Shi J J 2008 *Solid State Commun.* **145** 235
[19] Pokatilov E P, Nika D L and Balandin A A 2006 *Appl. Phys. Lett.* **89** 113508
[20] Tchernycheva M, Nevou L, Doyennette L, Julien F H, Warde E, Guillot F, Monroy E, Bellet-Amalric E, Remmele T and Albrecht M 2006 *Phys. Rev.* B **73** 125347
[21] van Capel P J S, Turchinovich D, Porte H P, Lahmann S, Rossow U, Hangleiter A and Dijkhuis J I 2011 *Phys. Rev.* B **84** 085317
[22] Komirenko S M, Kim K W, Stroscio M A and Dutta M 1999 *Phys. Rev.* B **59** 5013
[23] Lee B C, Kim K W, Stroscio M A and Dutta M 1998 *Phys. Rev.* B **58** 4860
[24] Zhu Y H and Shi J J 2009 *Physica* E **41** 746
[25] Zhao F Q and Zhang M 2011 *Int. J. Mod. Phys.* B **25** 2105
[26] Larsen D M 1964 *Phys. Rev.* **135** A419

[27] Larsen D M 1984 *Phys. Rev.* B **30** 4595
[28] Goldhana R, Scheiner J, Shokhovets S, Frey T, Köhler U, As D J and Lischka K 2000 *Appl. Phys. Lett.* **76** 291
[29] Vurgaftman I and Melyer J R 2003 *J. Appl. Phys.* **94** 3675
[30] Vurgaftman I, Meyer J R and Ram-Mohan L R 2001 *J. Appl. Phys.* **89** 5815
[31] Perlin P, Gorczyca I, Christensen N E, Grzegorg I, Teisseyre H and Suski T 1992 *Phys. Rev.* B **45** 13307
[32] Azuhata T, Sota T, Suzuki K and Nakamura S 1995 *J. Phys.*: *Condens. Matter* **7** L129
[33] Misek J and Srobar F 1979 *Electrotech. Cas.* **30** 690
[34] Harima H 2002 *J. Phys.*: *Condens. Matter* **14** R967
[35] Kim K, Lambrecht W R L and Segall B 1996 *Phys. Rev.* B **53** 16310
[36] Mora-Ramos M E 2001 *Phys. Stat. Sol.* (b) **223** 843
[37] Liang X X and Yang J S 1996 *Solid State Commun.* **100** 629
[38] Singleton J, Nicholas R J and Rogers D C 1988 *Surf. Sci.* **196** 429